

Determination of the Spectral Diffusion Kernel of a Protein by Single-Molecule Spectroscopy

Jürgen Baier,¹ Martin F. Richter,¹ Richard J. Cogdell,² Silke Oellerich,¹ and Jürgen Köhler¹

¹*Experimental Physics IV and BIMF, University of Bayreuth, 95440 Bayreuth, Germany*

²*Institute of Biomedical and Life Sciences, University of Glasgow, Glasgow G12 8QQ, United Kingdom*

(Received 15 June 2007; published 11 January 2008)

The spectral dynamics of individual bacterial light-harvesting-2 pigment-protein complexes have been studied at 1.4 K. The data provided the spectral diffusion kernel of the optical transitions of the embedded B800 bacteriochlorophyll *a* pigments. This kernel can be described by either a single Gaussian function or a superposition of Gaussian functions. Moreover, we found that the chromophores interact with two classes of TLSs that can be distinguished by their distance from the chromophore and are most likely located outside (class 1) and inside (class 2) the protein matrix.

DOI: [10.1103/PhysRevLett.100.018108](https://doi.org/10.1103/PhysRevLett.100.018108)

PACS numbers: 87.14.E-, 87.15.H-, 87.15.Ya

Although many proteins show well-resolved x-ray structures, their three-dimensional arrangement is often required to be rather flexible to discharge their biological functions [1]. This structural flexibility corresponds to rearrangements of their atoms and can be modeled by fluctuations of the proteins between different conformational substates [2,3]. Hence, proteins tend to feature a complicated potential energy surface with a large number of minima and a broad distribution of barriers. Even at low temperatures relaxation processes, i.e., transitions between these minima, give rise to rich dynamics covering many orders of magnitude in time [4]. Since the energies of the electronic energy levels of a chromophore that is embedded in a disordered host, such as a protein, are very sensitive to interactions with their local surroundings, optical spectroscopy provides a versatile tool to study the microscopic structure and relaxation dynamics of the host matrix via the spectral fluctuations (spectral diffusion) of the probe molecule. Numerous studies have been devoted to investigating the spectral diffusion of an optical transition of a chromophore embedded in a disordered matrix [5–10]. In hole-burning experiments such spectral fluctuations show up as waiting-time dependent line-broadening of the optical transition. Whereas in single-molecule experiments these spectral fluctuations can be directly observed either as spectral trails or random line shapes, depending on the time scales of the processes.

Because frozen solutions of proteins appear structurally random on a macroscopic scale their behavior has often been likened to that of a glass [11]. The standard model for the description of the dynamics of disordered materials relies on the assumption that structural changes are supposed to only occur in spatially localized regions, which can be characterized by double well potentials. At low temperatures these potentials are commonly approximated as two-level systems (TLSs) whose energies and tunneling matrix elements are randomly distributed [12,13].

However, in contrast to a chromophore embedded in a glass, the environment of a chromophore embedded in a protein is clearly hierarchically organized [14]. First, there

is the immediate protein-binding pocket of the chromophore, then there is the protein matrix, next there is the protein-solvent boundary, and finally there is the solvent. As a consequence of this it is very likely that this structural hierarchy imposes a spatial distribution of the TLSs which influences the various chromophore-TLS couplings as well [15]. Hence, it is not surprising that the dynamic laws that govern spectral diffusion in proteins are found to be different from those that govern it in glasses. In a previous paper [16] we were able to demonstrate that the standard TLS model for glasses fails to explain the spectral diffusion behavior of individual bacteriochlorophyll *a* (BChl *a*) molecules, which are naturally embedded in light-harvesting-2 (LH2) complexes from the purple bacterium *Rhodobacter (Rb.) sphaeroides*, strain 2.4.1. This pigment-protein complex serves as a peripheral light-harvesting antenna in bacterial photosynthesis and features a highly symmetric pigment assembly that comprises 27 BChl *a* molecules arranged in two concentric rings [17]. Eighteen closely interacting BChl *a* molecules (B850), which absorb at 850 nm ($11\,765\text{ cm}^{-1}$), constitute one ring, while nine well-separated BChl *a* pigments (B800) absorbing at about 800 nm ($12\,500\text{ cm}^{-1}$) form the second ring and act as sensitive probes for observing changes in their local protein environment. In this contribution we investigate in more detail the implications of the structural hierarchy and the imposed organization of the TLSs on the spectral diffusion behavior of the B800 chromophores.

A useful approach for the theoretical description of spectral diffusion is provided by the concept of the spectral diffusion kernel [18]. This can be defined as the conditional probability distribution that the absorption frequency of an optical transition is at frequency ν at time t if it was at frequency ν_0 at time t_0 . For the shape of the spectral diffusion kernel two limiting cases can be distinguished [19]. If the chromophore resides in a cavity that is comparable to or smaller than the average TLS-TLS distance; i.e., there are many TLSs close to the chromophore, and under the assumption of a dipole-dipole type interaction between the randomly distributed TLSs and the chromophore, the

shape of the spectral diffusion kernel of a distinct spectral line is Lorentzian. This corresponds to the standard TLS model for glasses and has been applied successfully to describe the temperature dependence of the specific heat of glasses and glasslike materials [20,21]. In the other limit, the chromophore resides in a cavity that is large with respect to the average TLS-TLS distance; i.e., there exists a minimum distance to the closest TLSs interacting with the chromophore. For this case the shape of the spectral diffusion kernel is Gaussian irrespective of the type of interaction potential [19]. Mathematically this prediction reflects the validity of the central limit theorem. The physical picture is that large spectral fluctuations are suppressed due to the lack of TLSs in the close vicinity of the chromophore.

The detergent-solubilized LH2 complexes of *Rb. sphaeroides* were prepared as described previously [22]. For the low-temperature single-molecule experiments a highly diluted solution of LH2 complexes was spin-coated onto a lithium-fluoride substrate and subsequently cooled down to 1.4 K in a helium-bath cryostat [8]. The individual, spatially isolated complexes were then excited by circularly polarized light from a continuous wave tunable Titanium:Sapphire laser and the fluorescence was detected by an avalanche photodiode (SPCM-AQR-16, EG&G). Long series of 1000–2000 spectra were recorded for five different complexes, with three different excitation intensities (5, 10, and 15 W/cm²). A similar experimental setup has been described in more detail in Ref. [23].

In the top part of Fig. 1(a) we show a stack of 2000 consecutively recorded fluorescence-excitation spectra from the B800 spectral region of an individual LH2 complex. The horizontal axis corresponds to the photon energy, the vertical axis to the scan number or equivalently to time, and the gray scale to the absorption intensity. The spectra were recorded with an excitation intensity of 10 W/cm² and the laser was scanned repeatedly with a scan speed of 44 cm⁻¹/s. The bottom part of Fig. 1(a) displays the fluorescence-excitation spectrum that results when all 2000 individual spectra are averaged. The sequential acquisition scheme allows to follow spectral variations of the absorptions in time as spectral trails. In Fig. 1(b) we show four examples for the distribution of the relative change in spectral position between two successive scans. The data for the upper histogram have been taken from the spectral trail boxed in Fig. 1(a), for the other histograms the spectral trails are not shown. Evidently, most events in the local environments of the chromophores lead to spectral changes in the order of 1–3 cm⁻¹, whereas only a few events give rise to spectral changes of about 7–10 cm⁻¹. Surprisingly, for LH2 from *Rb. sphaeroides* we did not observe spectral changes in the order of 100–200 cm⁻¹ as have been observed previously for the B800 chromophores in LH2 from *Rhodospirillum molischianum* [8,14].

In order to quantify the spectral diffusion behavior of the transitions we resort to the concept of spectral cumulants [24]. Therefore, we calculated the first spectral cumulant K_1 of a spectral feature, which is defined as $K_1 = M_1 - M_0$. Here M_0 refers to the frequency of the optical transition for a situation without any interaction between the

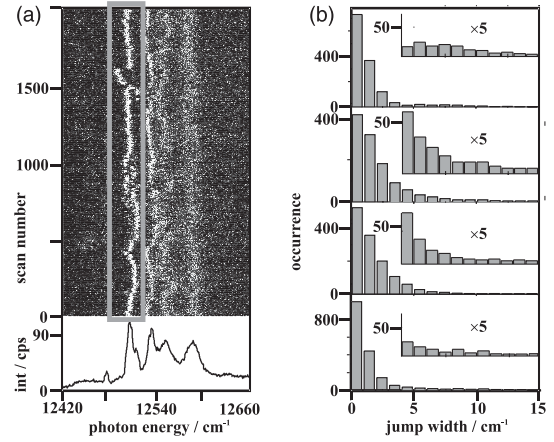


FIG. 1. (a) Top: two-dimensional representation of 2000 consecutively recorded fluorescence-excitation spectra from the B800 band of an individual LH2 complex from *Rb. sphaeroides* at 1.4 K. The horizontal axis corresponds to the photon energy, the vertical axis to the scan number or equivalently to time, and the gray scale to the absorption intensity. The spectra were recorded with an excitation intensity of 10 W/cm² and the laser was scanned repeatedly with a scan speed of 44 cm⁻¹/s. Bottom: Average over all fluorescence-excitation spectra in the stack. The intensity is given in counts per second (cps). (b) Histogram of the relative change in spectral position between two successive scans for four individual spectral trails. The upper histogram corresponds to the spectral feature boxed in (a), the other three histograms display data taken from different LH2 complexes. The insets show the frequency of spectral jumps larger than 4 cm⁻¹ on a scale that has been magnified by a factor of 5.

chromophore and its environment, and M_1 to the first spectral moment according to

$$M_1 = \frac{1}{I} \sum_i \nu_i I_i, \quad (1)$$

where I_i refers to the fluorescence intensity at data point i , ν_i to the photon energy at this spectral position, and I to the intensity of the complete spectrum. Unfortunately, the value of M_0 is experimentally not accessible. However, employing numerical simulations, it has been shown in Ref. [25] that the final result for K_1 is barely affected if instead of the vacuum frequency the spectral mean position of the transition is inserted for M_0 . Based on this approximation we calculated the distributions of the first cumulants for all spectral features studied. For the four examples displayed in Fig. 1(b) the distributions of K_1 are shown in Fig. 2. We have fitted the histograms by a sum of Gaussian distributions. The individual Gaussian distributions are shown as dashed lines and the sum is displayed as solid line in excellent agreement with the experimental data. In total we determined 23 histograms for the first cumulant. Their shapes were either compatible with a single Gaussian function (11 cases), with the sum of two Gaussian functions (9 cases), or the sum of three Gaussian functions (3

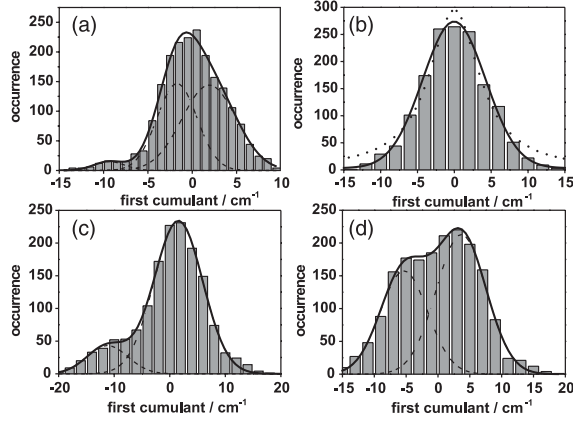


FIG. 2. Distributions of the first spectral cumulant for several individual absorptions. The dashed lines correspond to Gaussian fits, the solid line corresponds to the sum of the fitted Gaussian functions. The origin of the energy scale displays the spectral mean position of the spectral feature under study. (a), (b), (c), (d) show the cumulant histograms for the same spectral features that are analyzed in Fig. 1(b) (top to bottom). (a) The full widths at half maximum (FWHM) of the fitted Gaussian functions are 3.5 cm^{-1} , 4.5 cm^{-1} , and 6.1 cm^{-1} , respectively. The separations of the Gaussian functions are 7.7 cm^{-1} and 3.6 cm^{-1} (all from left to right). (b) The FWHM of the (single) fitted Gaussian function is 8.5 cm^{-1} . For illustration also a Lorentzian (dotted line) is fitted to the cumulant distribution. (c) The FWHMs of the fitted Gaussian functions are 8.8 cm^{-1} and 7.4 cm^{-1} , respectively, the separation is 12.8 cm^{-1} . (d) The FWHMs of the fitted Gaussian functions are 7.8 cm^{-1} and 7.4 cm^{-1} , respectively; the separation is 8.9 cm^{-1} .

cases). The full widths at half maximum (FWHM) of the fitted Gaussian functions were distributed between 3 cm^{-1} and 13 cm^{-1} with an average at 8 cm^{-1} . For the 12 cases that were fitted with two or three Gaussian functions the separation of the centers of the Gaussian shapes varied between 3 cm^{-1} and 12 cm^{-1} (average 7 cm^{-1}). Interestingly, none of the obtained histograms could adequately be described by a Lorentzian function [see Fig. 2(b), dotted line] or a sum of Lorentzian functions consistent with the results of the previous study [16].

Taking the definition of the spectral diffusion kernel into account and assigning ν_0 at t_0 to M_0 allows us to identify K_1 directly with the spectral diffusion kernel of the optical transition under study. Since all our experimentally obtained distributions of the first cumulant showed a very good agreement with Gaussian fits, we can safely conclude that the distribution of TLSs interacting with the probed chromophores cannot be described by the standard TLS model for glasses. The “chromophore in a cavity” limit appears more appropriate here, indicating the hierarchical organization of the environment that substantially differentiates this host system from synthetic polymers. Hence, the intriguing question arises whether it is possible to obtain an estimate for the minimum distance between the chromophore and the TLSs from our data. We approach

this issue by referencing to the results from pressure-dependent single-molecule experiments [26]. The idea is that the pressure-induced variations of the mutual distances and orientations of the chromophores will be comparable to those induced by conformational changes of the protein scaffold. In Ref. [27] it has been found that the pressure-induced spectral shift for a B800-chromophore in an LH2 complex is $0.1 \text{ cm}^{-1}/\text{MPa}$. In our experiments the minor spectral shifts of an absorption line between two successive scans are in the order of $1\text{--}3 \text{ cm}^{-1}$ [see Fig. 1(b)], which corresponds to a pressure of $20\text{--}30 \text{ MPa}$. Using the value of 0.1 GPa^{-1} for the compressibility of a protein [28] this translates into a relative distance change $\frac{\Delta R}{R}$ of some 10^{-3} . Upon changing the dipole moment of the TLS by $\Delta\mu_{\text{TLS}} = \Delta Rq$, where q refers to charge, one finds (according to the sudden jump model [29]) for an electronic dipole-dipole interaction between the chromophore and the TLS at distance R

$$\delta\nu = \frac{\mu\Delta\mu_{\text{TLS}}}{4\pi\epsilon_0 h R^3} = \frac{\mu}{4\pi\epsilon_0 h} \frac{\Delta R}{R} \frac{q}{R^2} \cong \frac{\mu}{4\pi\epsilon_0 h} 10^{-3} \frac{e}{R^2} \quad (2)$$

for the spectral shift of the chromophore transition. In Eq. (2) μ refers to the dipole moment of the chromophore (for BChl a $\mu = 2 \times 10^{-29} \text{ C m}$ [30] corresponding to 6 D). For a quantitative estimate of R we assumed $q \cong e$ to be in the order of an elementary charge. This results in $R \approx 1 \text{ nm}$ for the minimum distance between the chromophore and the TLS. From a similar calculation for the energetic splittings of the Gaussian contributions $\Delta\nu \approx 7\text{--}10 \text{ cm}^{-1}$ we arrive at a minimum chromophore-TLS distance of $R \approx 0.4 \text{ nm}$.

Relating the calculated distances to the geometrical arrangement of the B800 BChl a molecules in the binding pocket of LH2 (Fig. 3), leads to the following implications: First, TLSs at a distance of $\approx 1 \text{ nm}$ from the chromophore are very likely located outside the protein matrix. Therefore, we propose that the modulations of the transition frequencies of the chromophores in the order of a few wave numbers reflect the dynamics of the solvent, leading to the Gaussian shape of the contributions to the spectral diffusion kernel. Second, TLSs at distances from the chromophore of about 0.4 nm are most probably located inside the protein, leading to the energetic splitting of the Gaussian functions in the bi- or trimodal distributions. Since these larger spectral changes of about $7\text{--}10 \text{ cm}^{-1}$ occurred only for about 50% of the spectral features studied, we have to conclude that these types of TLSs are relatively rare—on the order of at most 1–2 per protein—which agrees with conclusions by the Friedrich group [15].

In summary, we have been able to record spectral diffusion trajectories of individual BChl a molecules embedded in the peripheral pigment-protein complex LH2 from *Rb. sphaeroides*. From these data we extracted the spectral diffusion kernel of the optical transitions, which featured in all cases a Gaussian shape or a superposition of Gaussian

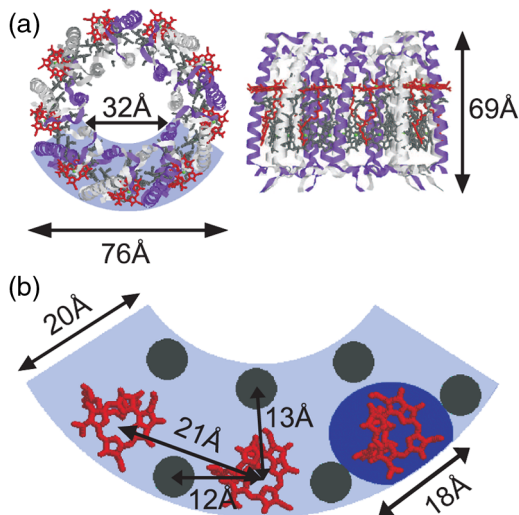


FIG. 3 (color online). (a) Top and side view of an LH2 complex. Because of the lack of a high-resolution x-ray structure for LH2 from *Rb. sphaeroides* the representation is based on the crystal structure of LH2 from *Rps. acidophila*. The shaded part is shown in greater detail in (b), which shows schematically three of the nine subunits. The B800 BChl *a* molecules are marked light gray (red), the protein helices are shown as gray dots. The dark gray (blue) area shows a binding pocket containing a B800 BChl *a* molecule.

functions. The shape of these distributions suggests a minimum distance between the chromophores and the TLSs that induce the spectral dynamics, whereas the necessity of superimposing two or three Gaussian functions indicates the presence of at least two populations of TLSs. From an order of magnitude calculation that is based on a dipole-dipole type interaction between the TLSs and the chromophore we find TLS-chromophore distances of 0.4 and 1 nm for the two classes of TLSs, respectively.

R.J.C thanks BBSRC for financial support. S.O. acknowledges a MC reintegration grant from the EU. Numerous fruitful discussions with Lothar Kador are gratefully acknowledged.

-
- [1] G.U. Nienhaus and R.D. Young, in *Encyclopedia of Applied Physics* edited by G.L. Trigg, E.H. Immergut, E. S. Vera, and W. Greulich (VCH Publishing, New York, 1996), Vol. 15, p. 163.
- [2] H. Frauenfelder, G.U. Nienhaus, and R.D. Young, *Disorder Effects on Relaxational Processes* (Springer-Verlag, Berlin, 1994), pp. 591–614.
- [3] H. Frauenfelder, S.G. Sligar, and P.G. Wolynes, *Science* **254**, 1598 (1991).

- [4] J. Schlichter, K.D. Fritsch, and J. Friedrich, *J. Mol. Liq.* **86**, 127 (2000).
- [5] S. Völker, *Annu. Rev. Phys. Chem.* **40**, 499 (1989).
- [6] H. Maier, B. Kharlamov, and D. Haarer, *Tunneling Systems in Amorphous and Crystalline Solids* (Springer-Verlag, Berlin, 1998), pp. 317–387.
- [7] A. Zumbusch, L. Fleury, R. Brown, and J.B.M. Orrit, *Phys. Rev. Lett.* **70**, 3584 (1993).
- [8] C. Hofmann, T.J. Aartsma, H. Michel, and J. Köhler, *New J. Phys.* **6**, 8 (2004).
- [9] F.L.H. Brown and R.J. Silbey, *J. Chem. Phys.* **108**, 7434 (1998).
- [10] W.P. Ambrose and W.E. Moerner, *Nature (London)* **349**, 225 (1991).
- [11] A. Ansari, J. Berendzen, S.F. Bowne, H. Frauenfelder, I.E.T. Iben, T.B. Sauke, E. Shyamsunder, and R.D. Young, *Proc. Natl. Acad. Sci. U.S.A.* **82**, 5000 (1985).
- [12] W.A. Phillips, *J. Low Temp. Phys.* **7**, 351 (1972).
- [13] P.W. Anderson, B.I. Halperin, and C.M. Varma, *Philos. Mag.* **25**, 1 (1972).
- [14] C. Hofmann, T.J. Aartsma, H. Michel, and J. Köhler, *Proc. Natl. Acad. Sci. U.S.A.* **100**, 15534 (2003).
- [15] J. Schlichter, J. Friedrich, L. Herenyi, and J. Fidy, *J. Chem. Phys.* **112**, 3045 (2000).
- [16] J. Baier, M.F. Richter, R.J. Cogdell, S. Oellerich, and J. Köhler, *J. Phys. Chem. B* **111**, 1135 (2007).
- [17] T. Walz, S.J. Jamieson, C.M. Bowers, P.A. Bullough, and C.N. Hunter, *J. Mol. Biol.* **282**, 833 (1998).
- [18] P.D. Reilly and J.L. Skinner, *J. Chem. Phys.* **101**, 965 (1994).
- [19] L. Kador, *J. Chem. Phys.* **95**, 5574 (1991).
- [20] R. Jankowiak, J.M. Hayes, and G.M. Small, *Phys. Rev. B* **38**, 2084 (1988).
- [21] W.A. Phillips, *Rep. Prog. Phys.* **50**, 1657 (1987).
- [22] R.J. Cogdell and A.M. Hawthornthwaite, in *The Photo Synthetic Reaction Center*, edited by J. Deisenhofer and J.R. Norris (Academic Press, San Diego, 1993), pp. 23–42.
- [23] E. Lang, J. Baier, and J. Köhler, *J. Microsc.* **222**, 118 (2006).
- [24] E. Barkai, A.V. Naumov, Y.G. Vainer, M. Bauer, and L. Kador, *Phys. Rev. Lett.* **91**, 075502 (2003).
- [25] A. Naumov, Y.G. Vainer, M. Bauer, and L. Kador, *J. Chem. Phys.* **116**, 8132 (2002).
- [26] R. Brown and M. Orrit, in *Single Molecule Optical Detection, Imaging and Spectroscopy*, edited by Th. Basché, W.E. Moerner, M. Orrit, and U.P.E. Wild (Verlag-Chemie, Munich, 1997), pp. 109–142.
- [27] V. Zazubovich, R. Jankowiak, and G.J. Small, *J. Phys. Chem. B* **106**, 6802 (2002).
- [28] J. Zollfrank and J. Friedrich, *J. Opt. Soc. Am. B* **9**, 956 (1992).
- [29] E. Geva and J.L. Skinner, *J. Phys. Chem. B* **101**, 8920 (1997).
- [30] R.G. Alden, E. Johnson, V. Nagarajan, W.W. Parson, C.J. Law, and R.J. Cogdell, *J. Phys. Chem. B* **101**, 4667 (1997).